Proceedings of the 7th JFPS International
Symposium on Fluid Power, TOYAMA 2008
September 15-18, 2008

P1-15

ANALYSES OF ELECTRIC AND FLOW FIELDS IN CHARGE INJECTION TYPE OF ELECTROSTATIC OIL FILTER

Khanh Duong TRAN*, Yu KOJIMA**, Yoshimasa TERASHITA*** and Hideki YANADA****

* Department of Mechanical & Structural System Engineering
Toyohashi University of Technology
** Panasonic Storage Battery Co.,Ltd.
555 Sakaijyuku, Kosai, 430-0452 Japan
*** Fuji Machine Mfg. Co., Ltd.
19 Chausuyama, Yamamachi, Chiryu, 472-8686 Japan
**** Department of Mechanical Engineering
Toyohashi University of Technology
1-1, Hibarigaoka, Tempaku-cho, Toyohashi, 441-8580 Japan
(E-mail: yanada@mech.tut.ac.jp)

ABSTRACT

This paper presents experimental and numerical simulation results of the electric and flow fields in a charge injection type of electrostatic oil filter. A previous work has shown that flow is generated from the tips of the projections of the emitter electrode towards the smooth electrodes because of ion drag phenomenon and that the flow may detach part of the contaminant particles captured on the smooth electrodes and may be the principal cause of the saturation of the filtration speed at higher applied voltages and oil temperatures. In order to minimize the bad influence of the ion drag flow on the filter performance, it is important to be able to predict the flow in filters of various configurations by numerical simulation. Experimental results of the flow field are compared to numerical simulation results. In addition, electric potential distribution is measured and is compared between experiment and simulation. It is shown that the magnitude of the ion drag flow is increased with increasing applied voltage, is decreased with decreasing electrode spacing and is larger for negative charge injection than for positive charge injection. Similar results can be obtained by numerical simulations but the improvement of simulation accuracy is necessary.

KEY WORDS

Electrostatic oil filter, Charge injection, Ion drag flow, EHD simulation,

NOMENCLATURE

D_i	: ion diffusivity
$\vec{E}$	: electric field
f_x, f_y	: Coulomb force
h	: height of projection
$\vec{j}$	: current density
p	: pressure
q	: charge density
s	: electrode spacing
T	: oil temperature
$\bar{u}$	: magnitude of ion drag flow

V : applied voltage
$\vec{V}$: velocity
x, y : x and y coordinates
ε : permittivity
μ : viscosity
μ_i : ionic mobility
ϕ : electric potential
ρ : mass density
σ : conductivity

INTRODUCTION

An electrostatic oil filter can remove submicrometer-sized contaminants such as the oxidation products of additives from oils. By virtue of this characteristic, it has contributed to lengthening the lives of lubricating oils and to decreasing waste oil as well as failures of machines including hydraulic systems [1,2]. However, the filtration speed of electrostatic oil filters is slow and it usually takes a long time for a contaminated oil to be purified.

Yanada and his coworkers [3,4] have proposed a new type of electrostatic oil filter, named charge injection type of electrostatic oil filter. The new filter uses one or more set(s) of an emitter electrode with many sharp projections and two smooth plate electrodes. The application of a high DC voltage between the emitter and smooth electrodes enables electric charges with the same polarity as that of the emitter electrode to be injected from the tips of the sharp projections into oils. If the electric charges injected can be adsorbed on the surfaces of the contaminants, the magnitude of Coulomb force exerted on them becomes larger and the contaminants may be easily removed from oils. It has been demonstrated using many types of oil that the filtration speed is increased to a great or some degree [3,4].

Previous investigation [5] has made clear the effects of mechanical factors such as the applied voltage, electrode spacing on the filtration speed. In addition, it has been shown that the filtration speed is apt to be saturated at higher applied voltages and oil temperatures. Observation of particle motion using a two-dimensional filter model has shown that oil flow caused from the tips of the sharp projections by the ion drag phenomenon may detach the contaminant particles from the surface of the smooth electrodes and that the ion drag flow is the primary cause of the saturation of the filtration speed [5]. In addition, in the previous investigation, only electrostatic field simulations were made to discuss the effect of the mechanical factors. If the flow field as well as the electric field in a filter can be predicted by numerical simulation, it will be helpful to design a filter with a better performance.

The ion drag phenomenon has been applied to ion drag pumps, heat transfer enhancement, etc. Numerical simulations of ion drag flow have been made but comparison between measured and simulated flow fields has hardly been done so far.

In this paper, using a two-dimensional filter model, the flow field and electric field are measured. In addition, numerical simulations are conducted and simulation results are compared with measured ones.

EXPERIMENTAL APPARATUS AND METHOD

Test oils

Two types of hydraulic fluids and a multipurpose oil were used for flow field observation. In Table 1, the values of the conductivity and viscosity of the test oils at 313K (40°C) are shown. Porous plastic particles, of which specific gravity is 1.02 and of which size ranges from 75 to 150 μm, were mixed into the test oils to visualize the ion drag flow. It was confirmed that the plastic particles were hardly charged in all the test oils and that the particle motion represented the motion of oil.

Table 1 Physical properties of test oils at 313K
(σ : conductivity, μ : viscosity)

Oil no.	σ (S/m)	μ (mPa•s)
1	1.24×10^{-10}	39.4
2	4.71×10^{-13}	27.1
3	2.48×10^{-9}	36.48

Observation of flow pattern

A schematic of the experimental apparatus used is shown in Figure 1. A test oil in reservoir ① is fed into the filter model ⑤ by a gear pump ③ and then returns to the reservoir. The oil in the reservoir is stirred by a magnetic stirrer ② to avoid the gravitational sedimentation of the plastic particles. A DC voltage is applied by a high DC power supply ⑥. The magnitude of the applied voltage was changed from 8kV up to 14kV in order to evaluate the effect of the applied voltage. The polarity of the applied DC voltage can be changed. The flow rate was adjusted to 2.19×10^{-6} m^3/s by an inverter ④. The temperature of the oil is controlled during the experiment by using a heater ⑦ and a thermoregulator ⑧. The motions of the particles were observed by a CCD camera ⑩ and the flow field was analyzed by a PIV technique using computer ⑪. In order to make the observation easy, approximately two-dimensional emitter electrodes were used as shown in Figure 2. The emitter electrodes are made of stainless steel and the rectangular projections were machined by laser beam. A transparent electrode was used as the smooth electrode for a plane light ⑨ to be penetrated

into the filter model, and is made of glass of which surface is coated by a conductive material (SnO_2). Emitter electrodes with different heights, h=5.5, 4.5 and 3.5mm, of the projection were made and the heights correspond to the electrode spacing of s=4, 5 and 6mm, respectively.

The magnitude of the applied voltage was varied from 8kV to 14kV while the electrode spacing was kept at s=4mm in order to investigate the effect of the applied voltage. When the ion drag flow was observed under different electrode spacings, the magnitude of the voltage was kept at 10kV. The oil temperature was kept at T= 313K.

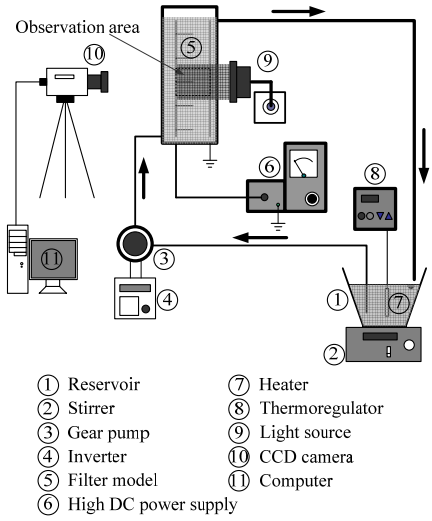

Figure 1 Schematic of apparatus used to observe ion drag flow

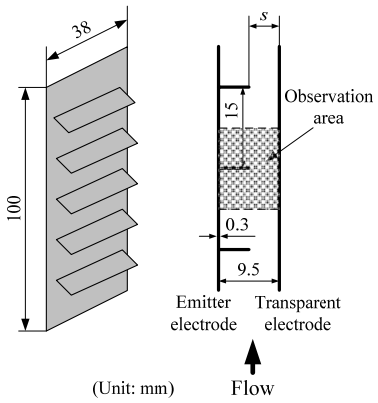

Figure 2 Schematic of two-dimensional emitter electrode

Measurement of electric potential distribution

In order to make clear the electric field between the electrodes, it is important to measure the electric potential distribution. Figure 3 shows a schematic of the apparatus used to measure the electric potential distribution. Because it takes a long time for the measured value at one point to be settled, the potential was measured only along the projection center line. A probe ⑥, which is made of stainless steel wire of 0.3 mm in diameter and is covered by a ceramic hollow tube of 1mm in outer diameter, is inserted between the electrodes and can be moved along the center line. The steel wire sticks out of the ceramic tube by 0.3mm as shown in Figure 3. The probe is connected to a circular plate ⑤ made of stainless steel. The electric potential of the circular plate is measured by using a surface potential meter ③ through a non-contacting probe ④. A DC voltage is supplied by a high voltage power supply ②.

In order to measure the electric potential distribution under different applied voltages, the electrode spacing was kept at s=5mm and the applied voltage was varied from 8kV to 14kV. The applied voltage was kept at V=10kV and electrode spacing was changed from 4 to 6 mm when examining the effect of the electrode spacing on the electric potential distribution.

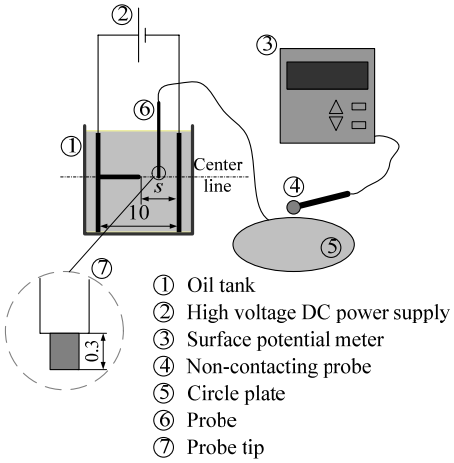

Figure 3 Schematic of apparatus used to measure electric potential distribution

NUMERICAL SIMULATION

In the simulations, two-dimensional, incompressible, steady, laminar flows are assumed. Because of relatively high viscosities of oils and relatively low flow velocities, the assumption of laminar flow is appropriate. Figure 4 shows the unit area to be analyzed. Taking the symmetry of the configuration into account, only a half of the observation area shown in Figure 2 was used for simulation. Followings are the basic equations that describe the flow field and electric field:

Continuity equation:

$$\frac{\partial u}{\partial x}+\frac{\partial v}{\partial y}=0 \tag{1}$$

Navier-Stokes' equation:

$$u\frac{\partial u}{\partial x}+v\frac{\partial u}{\partial y}=-\frac{1}{\rho}\frac{\partial p}{\partial x}+\frac{\mu}{\rho}\left(\frac{\partial^2 u}{\partial x^2}+\frac{\partial^2 u}{\partial y^2}\right)+f_x \tag{2}$$

$$u\frac{\partial v}{\partial x}+v\frac{\partial v}{\partial y}=-\frac{1}{\rho}\frac{\partial p}{\partial y}+\frac{\mu}{\rho}\left(\frac{\partial^2 v}{\partial x^2}+\frac{\partial^2 v}{\partial y^2}\right)+f_y \tag{3}$$

Charge conservation law:

$$\nabla \bullet \vec{j}=0 \tag{4}$$

Current density:

$$\vec{j}=q\mu_i\vec{E}+q\vec{V}-D_i\,\mathrm{grad}\,q \tag{5}$$

Gauss' law:

$$\frac{\partial^2\phi}{\partial x^2}+\frac{\partial^2\phi}{\partial y^2}=-\frac{q}{\varepsilon} \tag{6}$$

Coulomb force:

$$f_x=\frac{q}{\rho}E_x=-\frac{q}{\rho}\frac{\partial\phi}{\partial x} \tag{7}$$

$$f_y=\frac{q}{\rho}E_y=-\frac{q}{\rho}\frac{\partial\phi}{\partial y} \tag{8}$$

All the equations were discretized by a finite volume method and SIMPLE algorithm was used to solve the discretized equations.

In the numerical simulation of the ion drag flow, the injected charge density has to be given as a boundary condition but it cannot be theoretically known. In addition, it is known that at high electric fields, the ionic mobility does not obey the Walden's law and becomes significantly larger than that predicted by the Walden's law [6]. However, it has not been known how the ionic mobility depends on the electric field. In the simulations, the values of the injected charge density and the ionic mobility are found by trial and error for each test oil. It is assumed that charges are injected only from the surface of the projection tip (Figure 4) and that the amount of injected charges is proportional to the maximum electric field strength at the projection tip of electrostatic field.

RESULTS AND DISCUSSION

Examples of flow field obtained from experiment and simulation are shown in Figures 5 and 6, respectively. As can be seen from both figures, vortices are formed above and below the projection. The forms of the vortices are different to some degree between simulation and experiment but are relatively similar.

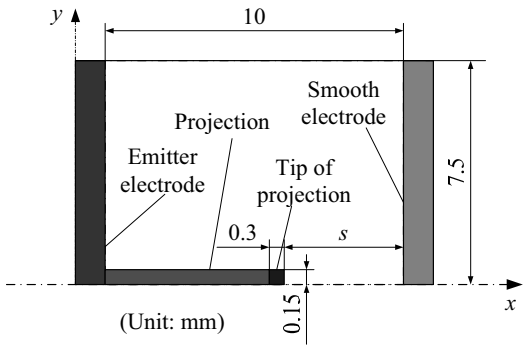

Figure 4 Example of unit area for numerical simulation

In order to evaluate the agreement between simulation and experiment, the velocity distribution in a slender rectangular region, shown in Figures 5 and 6, 0.5 mm above the projection is compared in Figure 7. It can be seen form Figure 7 that the maximum velocity is almost the same but that the velocity distribution in the simulation is not similar to that obtained by the experiment. The ion drag flow pattern is sometimes fluctuated with time and the electrode configuration is not exactly two-dimensional. In addition, the values of the injected charge density and the ionic mobility might not be necessarily appropriate. It is considered that those may be the causes of the difference between the experimental and simulation results.

Figure 8 and 9 show the effects of the applied voltage and the electrode spacing on the magnitude of the ion drag flow, respectively. In addition, comparisons between the experimental and simulation results are made. As described above, the flow is sometimes fluctuated and the measurement along or near the projection line was not easy. Therefore, the average magnitude of the velocity in the rectangular area shown in Figures 5 and 6 was used.

Figure 8 shows that the magnitude of the flow velocity increases with the increase in the magnitude of the applied voltage. The magnitude of the flow velocity increases almost linearly in the simulation. This is because the amount of the injected charge density was assumed to be proportional to the maximum electric field strength at the projection tip for electrostatic field.

Figure 9 shows that the increase in the electrode spacing brings about a larger ion drag flow velocity. The increasing tendency of the velocity in the simulation is the same as the experiment, but the magnitude is lower.

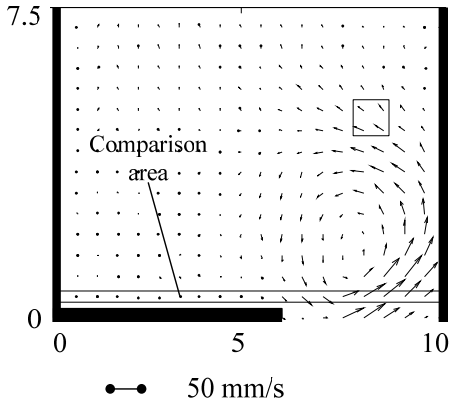

Figure 5 Example of measured flow field
(Oil 1, V=+10kV, s = 4mm, T=313K)

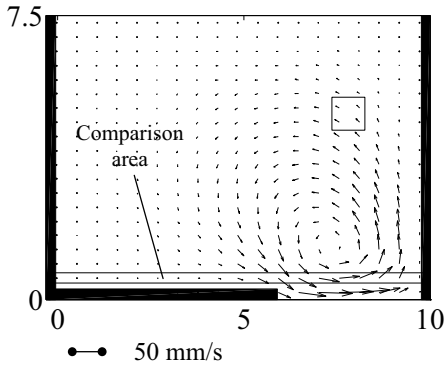

Figure 6 Example of computed flow field
(Oil 1, V= 10kV, s = 4mm, T=313K)

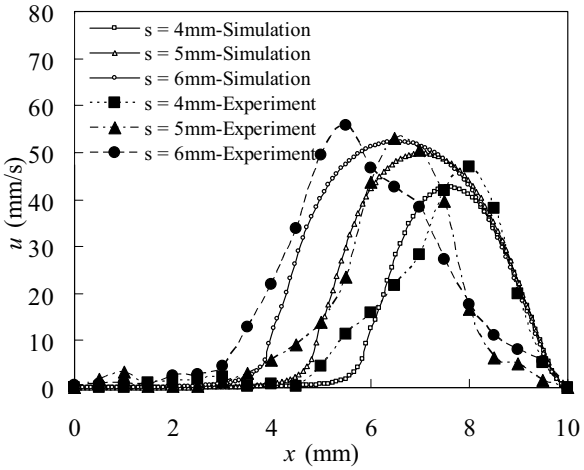

Figure 7 Comparison of velocity distribution between experiment and simulation for oil 1

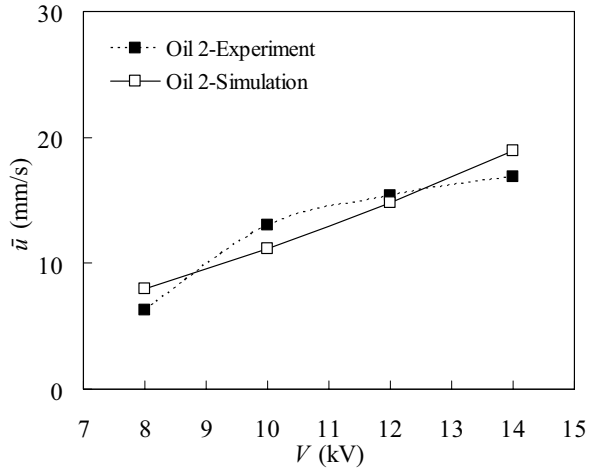

Figure 8 Effect of applied voltage on ion drag flow
(s=5mm, T=313K)

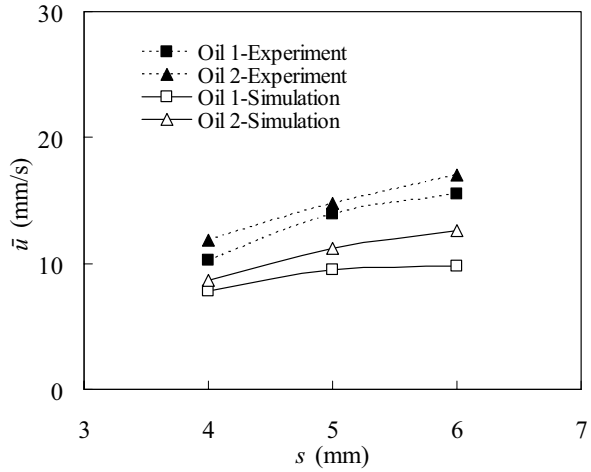

Figure 9 Effect of electrode spacing on ion drag flow
(V=+10kV; T= 313K)

The polarity of the charge injection also affects the ion drag flow as shown in Figure 10. The magnitude of the flow velocity increases with increasing applied voltage more strongly for the negative charge injection than for the positive one. It has been shown that negative charges are more easily injected than positive ones [4]. It has been pointed out that the ion drag flow may prevent contaminant particles from being captured on the smooth electrodes [5]. Therefore, when in particular injecting negative charges, some measures to minimize the bad influence of the ion drag flow have to be taken. This is the subject for a future study.

The results of the measurement and simulation of the electric potential distribution for different applied voltages for oil 2 are shown in Figure 11. The potential

is monotonously decreased from the projection tip to the smooth electrode for the simulation while bumps appear between the electrodes in the measured potential distribution curves. Such difference may arise from inappropriate values of the injected charge density and ionic mobility and the elucidation of the cause of the difference is also the subject for a future study. Similar potential distributions to Figure 11 were obtained for the other test oils.

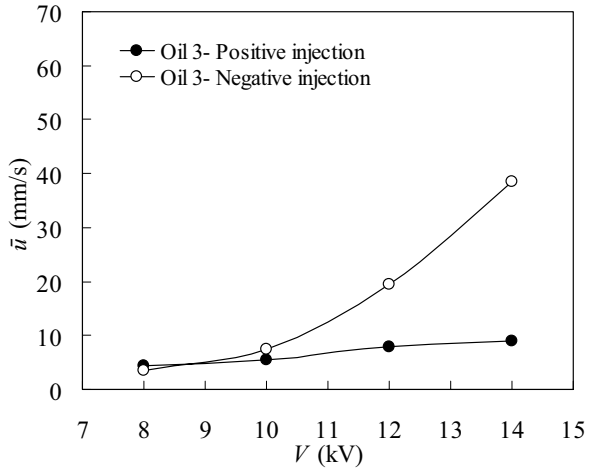

Figure 10 Effect of applied voltage polarity on ion drag flow (oil 3, s=5mm, T=313K)

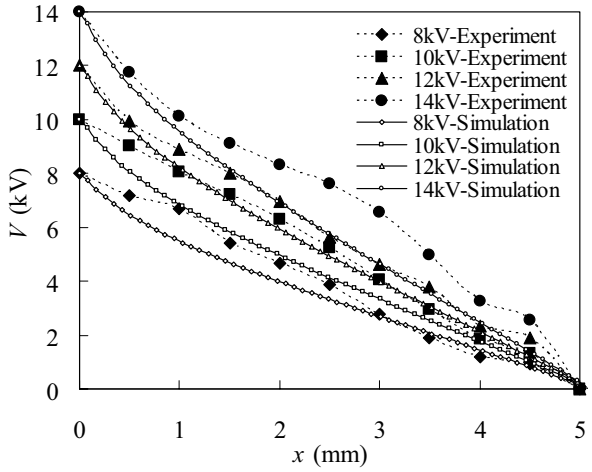

Figure 11 Effect of applied voltage on electric potential distribution (oil 2, s=5mm)

CONCLUSIONS

In this paper, ion drag flow field and electric field in a charge injection type of electrostatic oil filter were examined by experiment and numerical simulation. It was shown that the magnitude of the ion drag flow is increased with increasing applied voltage and decreased with decreasing electrode spacing and that those results can be obtained also by numerical simulation, though the simulation accuracy is not very good. In order to improve the simulation accuracy, the dependences of the injected charge density and the ionic mobility on the electric field strength need to be found out.

ACKNOWLEDGEMENT

The authors would like to express their gratitude to Mr. Y. Asai for his help in part of the experiments and simulations. This work was financially supported by the Japan Society for the Promotion of Science through the Grant-in-Aid for Scientific Research (C) (No. 18560132).

REFERENCES

1. Tobisu, T., Separation technology---electrostatic oil cleaner (in Japanese), J. Japan Soc. Lubric. Engrs., 1984, **29**-12, pp.881-884.(in Japanese)
2. Sasaki, A., Sasaoka, M., Tobisu, T., Uchiyama, S., and Sasaki, T., The use of electrostatic liquid cleaning for contamination control of hydraulic oil, Lubric. Engng, 1988, **44**-3, pp.251-256.
3. Yanada, H., Masuoka, T. and Yoshida, Y., Fundamental investigation of charge-injection type of electrostatic oil filter, The 1st Int. Conf. Manufacturing, Machine Design and Tribology 2005, Seoul, Korea (2005), CD-ROM.
4. Yanada, H. and Tran, K. D., Fundamental investigation of charge injection type of electrostatic oil filter, J. Advanced Mechanical Design, Systems, and Manufacturing, 2008, **2**-1, pp.119-132.
5. Tran, K. D. and Yanada, H., Fundamental Investigation of Charge Injection Type of Electrostatic Oil Filter (Effects of Mechanical Factors on Filtration Speed), J. Advanced Mechanical Design, Systems, and Manufacturing (2008), (submitted)
6. Felici, N. J., D.C. conduction in liquid dielectrics - A survey of recent progress (part I), Direct Current, 1972, **2**-3, pp.90-99.